Design of a GaN Based Integrated Modular Motor Drive

M. Uğur, O. Keysan

Abstract -- **In this study, design procedure of an Integrated Modular Motor Drive (IMMD) is presented focusing on high power density. The design is based on a permanent magnet synchronous motor (PMSM) and GaN FETs. Fractional slot concentrated windings are used on the stator. Slot/pole combination and winding configuration is selected based on having low cogging torque and high winding factor. An extended motor drive inverter topology is proposed where 2-level voltage source inverters are connected both in series and parallel. Optimum selection of number of modules is discussed and power semiconductor devices are selected based on loss characterization. Optimum DC link capacitor bank is determined and the effect of interleaving is investigated. The performance of the motor is validated with ANSYS/Maxwell simulations. Motor drive performance is obtained with MATLAB/Simulink simulations. The efficiency of the motor drive is enhanced by 2% compared to a conventional motor drive. An overall system power density over 1 kW/lt has been achieved with the proposed series/parallel motor drive configuration having GaN FETs.**

Index Terms—**Gallium nitride, Integrated motor drive, Modular motor, Permanent magnet synchronous motor, Power density**

I. Introduction

In conventional motor drive systems, the drive units are placed in separate cabinets which increases the overall weight and volume and decreases the power density of the system. Furthermore, the drive units are connected to the motor by means of long cables which cause transient voltage overshoots due to the high frequency pulse width modulation (PWM) operation.

A novel concept called Integrated Modular Motor Drives (IMMDs) has been proposed suggesting that all the components of the motor drive system can be integrated onto the motor including power electronics, control electronics, passive components and heat sink [1]. By doing so, the power density of the system can be enhanced significantly which is very critical in aerospace and electric traction applications [2], [3]. In addition, cost reduction up to 20% is possible thanks to the elimination of enclosures and connection equipment [1]. The absence of connection cables yields less leakage current on the winding insulation which will extend the lifespan of the motor as well as minimize electromagnetic interference (EMI) problems [4].

With modularization, the overall system is segmented with modules sharing the total power equally. By this way, the fault tolerance of the system is increased [2]. The current and voltage stress on the power semiconductor devices can also be decreased by modularization. Moreover, the components which produce heat due to power loss are distributed in a wider surface area which makes the thermal design more convenient as well as decreases the chance of hot spots. Finally, the manufacturing, installation and maintenance costs decrease thanks to the modular structure [1].

However, integration of the motor and drive brings several challenges. Firstly, fitting all the drive components to the available space requires size optimization and careful layout design [4]. Secondly, it is difficult to cool the motor and drive simultaneously since they both produce heat. Furthermore, all the electronic components are subjected to a higher ambient temperature and continuous vibration and should be selected accordingly [5].

To overcome these challenges, it has been proposed in the literature that wide band gap (WBG) power semiconductor devices such as Gallium Nitride (GaN) can be used which are capable of operating at high frequencies [4]. By doing so, the size of the passive components can be reduced with acceptable heat sink size thanks to superior efficiency of GaN based converters compared to conventional ones [6]. However, high frequency operation highlights the impact of parasitic components on the power stage and gate drive circuits which makes layout design critical.

In this paper, design of an IMMD system is presented with enhanced power density, increased efficiency and enhanced fault tolerance capability. A detailed design procedure is given for both motor and the drive and the resultant design parameters are verified by ANSYS/Maxwell and MATLAB/Simulink simulations. Comparison of the IMMD performance with a conventional counterpart having IGBTs is also provided. In Section 2, basic structure and current technology prospects of IMMDs are introduced. In section 3, design of the system including the motor and the drive is explained. In section 4, simulation results are presented and in section 5, conclusions are given.

II. Basic Structure of IMMD

There are several types of integration of the motor drive into the motor. In this paper, integration into the stator back iron is considered, which also allows the modularization of the

This work was supported by the Scientific and Technological Research Council of Turkey (TUBITAK) under the TUBITAK project number 117E252.

Mesut Uğur is with the Department of Electrical and Electronics Engineering, Middle East Technical University, Ankara, 06800, TURKEY (e-mail: mesut.ugur@metu.edu.tr).

Ozan Keysan is with the Department of Electrical and Electronics Engineering, Middle East Technical University, Ankara, 06800, TURKEY (e-mail: keysan@metu.edu.tr).

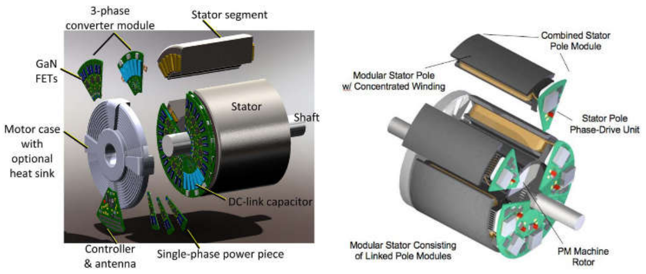

Fig. 1. IMMD prototype examples with stator back-iron integration [4], [7]

system. In this configuration, one module is composed of a stator pole piece, a concentrated coil and a power converter dedicated to its own winding along with its controller [5]. Two prototype examples of such a structure from the literature are shown in Fig. 1 [4], [7].

In conventional (non-modular) motors, each stator coil belonging to different pole pairs on the stator are usually connected in series to form one phase of the stator. On the other hand, the windings in different poles can be connected to separate motor drive units in modular motors. These types of motors are called split-winding machines [8], as the redundancy and fault tolerance of the system is enhanced thanks to this modularization. Moreover, the motor drive modules can be connected with different configurations which makes the design more flexible.

A general block diagram of one module of an IMMD system is shown in Fig. 2 [5], in which concentrated windings are preferred for their easy manufacturing and suitability for split-winding stators, especially in modular motors. Fractional slot concentrated winding (FSCW) permanent magnet synchronous motors (PMSMs) are very common in IMMD studies thanks to their high torque density, low torque ripple and fault tolerance capability [9].

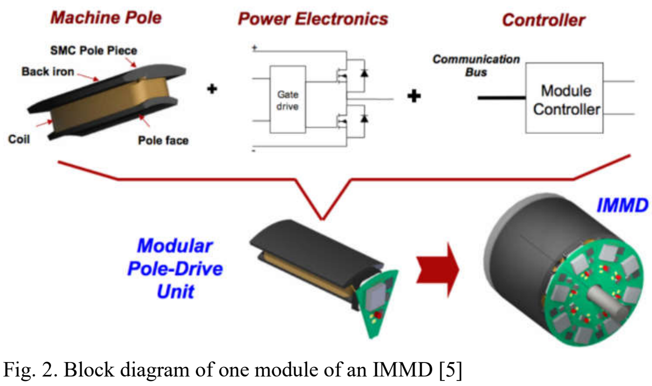

Fig. 2. Block diagram of one module of an IMMD [5]

As for the power electronics, many different topologies have been proposed for AC motor drive systems such as, 2-level voltage source inverter (VSI), multilevel neutral point clamped (NPC) VSI, multilevel flying capacitor (FC) VSI, cascaded H-bridge (CHB) etc. [8]. As mentioned previously, for a modular motor drive, several other motor drive topologies become available thanks to the design flexibility. Connection of separate 2-level VSIs in series or parallel are shown in Fig. 3, with a conventional motor drive [10]. Furthermore, the aforementioned topologies can also be connected in series and/or parallel on the DC link to form a new topology. These types of connections are possible thanks to the fact that the windings, which are split and hence electrically isolated, do not cause any in-circulating currents between the inverter modules. The major advantage of this possibility is to be able to split the voltage and/or current requirement of each inverter. One practical usage of this fact is making low voltage power semiconductor device viable such as GaN transistors by dividing the DC link voltage.

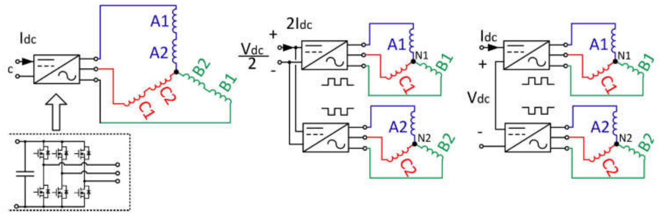

(a) Conventional (b) Parallel (c) Series

Fig. 3. Different motor drive connections for a modular motor [10]

Employment of GaN transistors is especially crucial for IMMDs , as these devices have much higher switching speeds compared to conventional silicon based devices such as IGBTs and admissible on-state losses which make them more efficient [11]. Moreover, they can withstand to higher junction temperatures. The volumes of the integrated motor drives can be reduced by utilizing GaNs thanks to their higher efficiency which makes cooling easier, and higher switching frequencies reducing the size of passive components. In high power applications, the maximum switching frequency for an IGBT device is limited to 20 kHz, whereas the switching frequency of GaNs can go up to 100 kHz in applications with kW range [11]. As a matter of fact, although IGBTs were used in the early IMMD prototypes [5], [7], the latest IMMD prototypes utilize GaNs FETs as power semiconductor devices [4].

Selection of DC bus capacitors is also critical in integrated drives in terms of power density as they usually constitute more than 20% of the motor drive system volume and 30% of the motor drive system weight [6]. Moreover, the height of the motor drive is mostly determined by these capacitors [4]. In conventional motor drives, aluminum electrolytic type capacitors are mostly used thanks to their low cost and high capacitance per volume. However, they have relatively low RMS current handling capability per unit volume and relatively shorter lifetime which is also dependent on the operating parameters [6]. Metal film type capacitors are better in terms of RMS current ratings, lifetime and reliability. However, their capacitance per volume is lower. It is possible to reduce the capacitance requirement by several means such as increasing the switching frequency and interleaving. Therefore, using metallized polypropylene film capacitors in the DC bus of integrated motor drives results in smaller motor drive volumes.

III. Design of the IMMD System

The design process of the IMMD system can be divided into two parts: design of the motor and design of the drive. The design is based on an input circuit having a passive diode bridge rectifier with an LC DC link pre-filter. The effects of this rectifier module are out of the scope of this study. The machine is a 3-phase low speed PMSM having a modular stator with fractional slot concentrated winding. The system parameters used in the design process are presented in Table 1.

The first parameter to be decided is the total number of 2-level voltage source inverter (2L-VSI) modules. As stated before, the number of series or parallel connected modules can be varied according to the voltage and current requirements and the system parameters such as the DC link voltage and total output power. It has also been specified that GaN transistors are used to reach to the efficiency and power density target. However, the maximum blocking voltage ratings of the currently available GaN transistors is 650V [11]. In case of 2L-VSIs are used, the required minimum power semiconductor blocking voltage should be higher than the nominal DC link voltage (540V) with at least 30% safety margin considering possible voltage overshoot effects due to parasitic inductances and high switching speed of GaN FETs, and possible swell or overvoltage events on the grid side. It is clear that, at least two series modules should be used with the aforementioned GaN devices to reduce the voltage per transistor below 650V. The total number of modules become an even number when the number of series connection is two.

There are a few parameters which affect the number of parallel connected modules. One of them is the required power rating of each module which effect the current ratings of the semiconductor devices and the drive efficiency. Another one is the number of stator slots. Instead of number of stator slots per pole per phase (q_s) which is a common factor for conventional systems, number of stator slots per module per phase (w_s) is introduced in this paper. For a double layer stator winding, w_s can be selected as an even number. For example, for an IMMD having 2 series and 3 parallel modules, and 2 stator slots per module per phase, the number of stator slots (Q_s) turns out to be 36.

Finally, the effect of interleaving and its utilization for minimization of DC link capacitor bank size is considered to determine the number of modules. In [6], the effect of the number of modules and applied interleaving angle to the current ripple on the DC link capacitor bank is studied for an IMMD, and it has been shown that selecting four modules gives the best result in terms of DC link capacitor size. Using that result, it is decided to use a total number of 4 modules which are connected in 2-series and 2-parallel configuration. The schematic diagram of the suggested IMMD system topology is shown in Fig. 4.

TABLE I
THE SYSTEM PARAMETERS USED IN THE IMMD DESIGN PROCESS

Parameter	Value
Total output power, P_{out}	8 kW
Rated speed, N_r	600 rpm
DC link voltage, V_{dc}	540 V
Motor efficiency aim, $\eta_{m,a}$	96%
Drive efficiency aim, $\eta_{d,a}$	98%

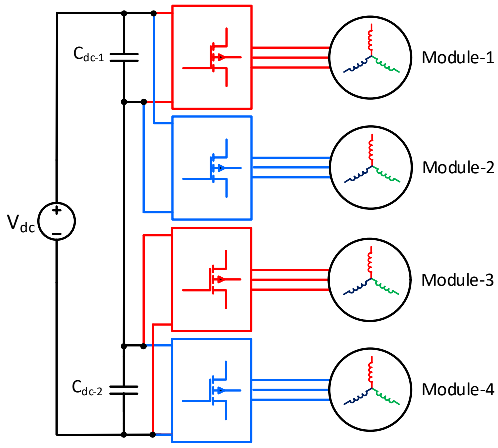

Fig. 4. Schematic diagram of the suggested IMMD topology with 2-series and 2-parallel 2-level VSIs

A. Determination of the Motor Parameters

The main dimensions of the motor are determined according to the torque requirement (T_m) and shear stress (σ) using magnetic loading (B) and electrical loading (A) limits selected for the IMMD application, as expressed in (1). V_m is the motor air gap volume as shown in (2), where D_{is} is the air gap (bore) diameter and L_a is the axial length of the motor. The aspect ratio, which is the ratio of the axial length to the bore diameter is selected as 0.75 for this application. The number of slots should be an integer multiple of 24 since the number of 3-phase modules is 4. For the given dimensions, increasing the number of slots per module per phase makes the outer diameter too large. It has been observed that better results in terms of copper fill factor are achieved when w_s is 2. Moreover, the number of rotor poles is selected as 20 by using previously obtained winding factor tables for different slot/pole combinations [9].

The number of turns per coil side can be determined by the induced voltage requirement of each phase on each module, which can be expressed as in (3), in rms, where $N_{ph\text{-}m}$ is number of turns per phase per module, f_s is the applied fundamental frequency at rated conditions, Φ_{pp} is the flux under a pole and k_w is the fundamental winding factor. The flux per pole can be calculated using the machine dimensions and air gap flux density (B_g) as in (4), where p is the number of rotor poles. The winding factor is determined using the pre-calculated tables created for fractional slot machines in terms of slot/pole combinations as 0.933 [9]. The fundamental frequency is determined by the rated speed and pole number of the synchronous motor, as in (5). Assuming that the motor drive inverters are switched with sinusoidal pulse width modulation (SPWM) technique, the terminal voltage of one phase of each module is determined using (6), where m_a is the modulation index and $V_{dc\text{-}m}$ is the nominal DC link voltage on one module. The required number of turns per coil side, z_{Q1} equal to 40 using (7), where l is the number of layers.

Obtained motor parameters are shown in Table 2. In Fig. 5, the proposed winding diagram per module is shown. The main purpose behind the selection is having large enough winding factor while keeping the space harmonic content low.

$$T_m = 2\,\sigma\,V_m = 2\,B_{avg}\,A_{rms}\,V_m \quad (1)$$

$$V_m = \pi\,D_{is}^{\,2}\,L_a/4 \quad (2)$$

$$E_{ph-m} = 4.44\,N_{ph-m}\,f_s\,\Phi_{pp}\,k_w \quad (3)$$

$$\Phi_{pp} = 2\,D_{is}\,L_a\,B_g/p \quad (4)$$

$$f_s = N_m\,p\,/120 \quad (5)$$

$$V_{ph-m} = m_a\,V_{dc-m}/2\sqrt{2} \quad (6)$$

$$z_Q = 2\,N_{ph-m}/w_s\,l \quad (7)$$

TABLE II
THE RESULTANT MOTOR PARAMETERS

Parameter	Value
Number of stator slots, Q_s	24
Number of rotor poles, p	20
Motor axial length, L_a	135 mm
Stator outer diameter, D_{os}	270 mm
Stator inner diameter, D_{is}	180 mm
Air gap length, l_g	1.5 mm
Magnet thickness, l_m	5.5 mm
Number of turns per coil side, z_Q	40
Stator fill factor, k_{cu}	0.4
Stator winding factor, k_{ws}	0.933

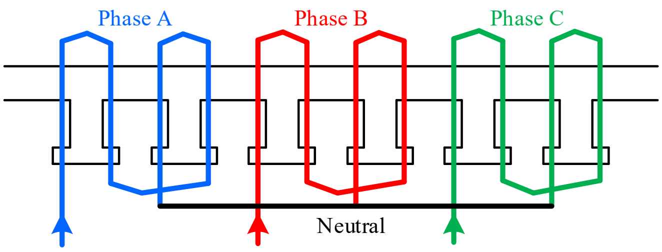

Fig. 5. Proposed winding diagram of one module

B. Design of the Drive Parameters

Power semiconductor devices are chosen according to voltage and current requirements. Among the suitable alternatives, motor drive efficiency is the main concern for device selection. The voltage requirement of each device has already been established. There are two GaN transistor types which have breakdown voltage ratings as high as 650V, cascade GaNs manufactured by Transphorm and enhancement mode (e-mode) GaNs manufactured by GaN Systems [11]. The next step is to determine the current rating. By using the phase voltage calculated in the previous step, the phase current of each module can be found using (8).

$$I_{ph-m} = P_{out-m}\,/\,\left[3\,\eta_m\,\cos(\varphi)\,f_s\,V_{ph-m}\right] \quad (8)$$

One device from each type is selected having similar ratings along with an IGBT for comparison purposes, as shown in Table 3 [11]. Power semiconductor device losses can be categorized as transistor forward conduction loss (P_{tc}), transistor switching loss (P_{ts}), transistor reverse conduction loss (anti-parallel diode conduction loss for IGBT case, P_{dc}) and loss on C_{oss} capacitance (P_{oss}) or diode reverse recovery loss for IGBT case, (P_{dr}). The analytical model used in the loss calculations is shown in (9)-(15). An approximate method which is well-established and commonly used for sinusoidal motor drive inverters is utilized to simplify the analysis. In this model, I_{cp} and I_{ep} are the forward and reverse peak currents, respectively, f_{sw} is the switching frequency, φ is the power factor angle, E_{on}, E_{off} and E_{oss} stand for turn-on, turn-off and C_{oss} energies, $V_{ce\text{-}sat}$ is saturation voltage drop for the IGBT, $R_{ds\text{-}on}$ is the on-state resistance for GaN, V_{ec} is the reverse voltage drop for the diode, I_{rr} and t_{rr} are the diode reverse recovery current and time, respectively, and $V_{ce\text{-}p}$ is the reverse recovery peak voltage.

$$P_{tc} = I_{cp}\,V_{ce-sat}\,[1/8 + m_a\cos(\varphi)/3\,\pi]\,(IGBT) \quad (9)$$

$$P_{tc} = I_{dp}^{\,2}\,R_{ds-on}\,[1/8 + m_a\cos(\varphi)/3\,\pi]\,(GaN) \quad (10)$$

$$P_{ts} = \left(E_{on} + E_{off}\right)[f_{sw}/\pi] \quad (11)$$

$$P_{dc} = I_{ep}\,V_{ec}\,[1/8 - m_a\cos(\varphi)/3\,\pi]\,(IGBT) \quad (12)$$

$$P_{dc} = I_{sp}^{\,2}\,R_{ds-on}\,[1/8 - m_a\cos(\varphi)/3\,\pi]\,(GaN) \quad (13)$$

$$P_{oss} = E_{oss}\,f_{sw}\,/\,\pi \quad (14)$$

$$P_{dr} = I_{rr}\,t_{rr}\,V_{ce-p}\,[f_{sw}/8] \quad (15)$$

TABLE III
ALTERNATIVE COMMERCIAL TRANSISTORS [11]

Device	**FP35R12KT4P**	**TPH3205WSB**	**GS66508B**
Type	IGBT	Cascode GaN	E-mode GaN
Manufacturer	Infineon	Transphorm	GaN systems
Voltage	1200 V	650 V	650 V
Current	35 A	35 A	30 A
$V_{ce,sat}$	2,15 V	-	-
$R_{ds,on}$	-	60 mΩ	50 mΩ

Selection of the DC bus capacitors is performed for the designed system using metal film type capacitors. In order to compare the IMMD design with a conventional motor drive in terms of power density, the same design procedure is also applied to the conventional drive with IGBTs. The parameters affecting the capacitor selection are DC voltage (V_{dc}), capacitance requirement to meet the voltage ripple constraint (C_{dc}), the current requirement due to the RMS rating of capacitor bank current ripple ($I_{c,rms}$) and temperature rise of each capacitor (T_{core}). The analytical model used for these parameters are shown in (16)-(19), where $V_{dc\text{-}r}$ is the maximum allowed peak-to-peak voltage ripple in percent, T_a is the ambient temperature, P_c is the power loss on capacitor which is also dependent on core temperature, $R_{th\text{-}c}$ is the thermal resistance of the capacitor and R_c is the ESR value of the capacitors [6], [12].

$$C_{dc} = \frac{m_a\,I_{s,rms}}{16\,V_{dc-r}\,f_{sw}}\sqrt{\left(6 - \frac{96\sqrt{3}m_a}{5\pi} + \frac{9{m_a}^2}{2}\right)(\cos\varphi)^2 + \frac{8\sqrt{3}m_a}{5\pi}} \quad (16)$$

$$I_{c,rms} = I_{s,rms}\sqrt{2\,m_a\left(\frac{\sqrt{3}}{4\pi} + (\cos\varphi)^2\left(\frac{\sqrt{3}}{\pi} - \frac{9m_a}{16}\right)\right)} \quad (17)$$

$$T_{core} = T_a + P_c(T_{core})\,R_{th,c} \quad (18)$$

$$P_c = I_{c,rms}^{\,2}\,R_c(T_{core}) \quad (19)$$

IV. Simulation Results

The performance of the motor is analyzed using ANSYS/Maxwell simulation environment. The analytical results are shown in Table 4 which have been obtained via the RMxprt tool of Maxwell software. The designed motor is also simulated using 2D FEM analysis tool to obtain transient characteristics. The phase induced voltage, current waveforms and machine torque are presented in Figs. 6, 7 and 8, respectively. The flux density distribution of one module is shown in Fig. 9. The torque ripple and cogging torque values are below the specified limits.

TABLE IV
MOTOR SIMULATION RESULTS (RMXPRT)

Parameter	Value	Parameter	Value
$E_{ph\text{-}m}$	85 V_{rms}	J_{rms}	3.9 A/mm^2
$I_{ph\text{-}m}$	8.8 A_{rms}	P_{cu}	229 W
T_m	133 Nm	P_{core}	97 W
k_{fill}	47 %	η_m	95.9 %

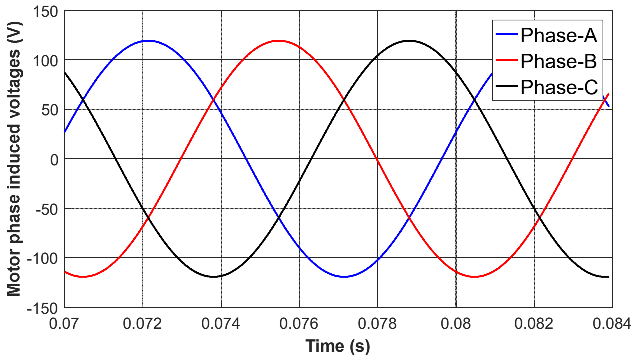

Fig. 6. Induced phase voltages (2D FEM analysis)

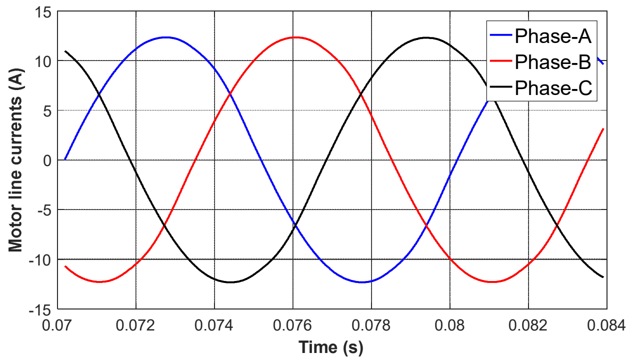

Fig. 7. Line currents of one module (2D FEM analysis)

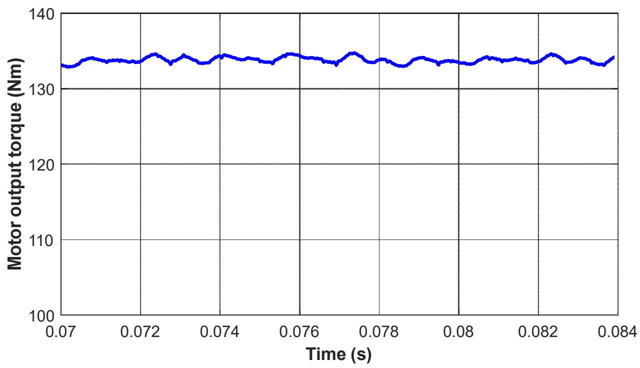

Fig. 8. Motor output torque (2D FEM analysis) *(Torque ripple: 1.25%)*

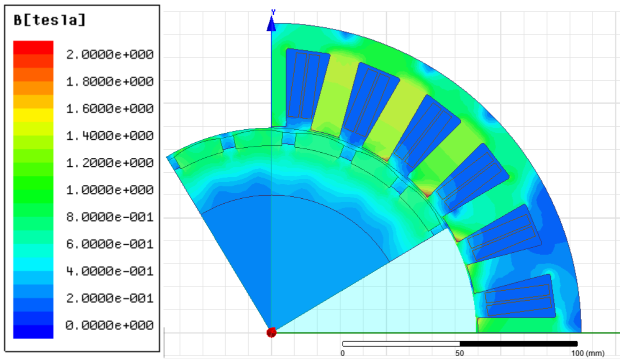

Fig. 9. Flux density distribution over one module

Drive loss is analyzed using the model presented in (9)-(15), which includes the selected devices with a conventional system having IGBTs and two IMMD systems with different types of GaNs. The losses are compared in Fig. 10. The results show that, even with a switching frequency five times higher than IGBTs, the total system loss is halved with GaN devices. The switching frequency of IGBT simulations are limited to 20 kHz, due to the practical limitations of those devices. It is observed that the main loss reduction with GaN devices is on the switching loss part, as expected. However, transistor conduction losses are a little bit higher with GaNs, although reverse conduction losses are similar. There are two main reasons for this. Firstly, IGBT conduction performance in high current applications is good. However, the GaN technology has not been proven itself in terms of on-state voltage drop, while it has developed to have similar performance. Secondly, the IMMD system has 2-series structure so that each module carries two times the current they would have when there are 4 parallel modules. In conclusion, both cascade and e-mode GaN FETs reach 98% drive efficiencies at 100 kHz switching frequency. Despite the superior efficiencies, motor drives having high speed GaN FETs are problematic due to high dv/dt rates which may damage the motor insulation. Therefore, LC filters between the drive inverters and motor windings may be required.

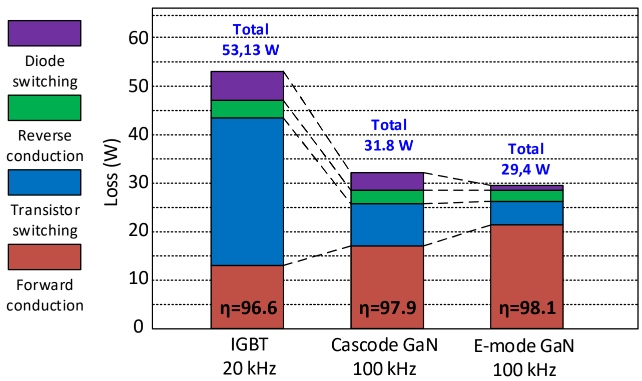

Fig. 10. Comparative loss analysis having a conventional system with IGBT and two different IMMD systems with GaN

Motor drive simulations are performed using 4 modules with the proposed configuration. DC link capacitors are selected resulting in 1% voltage ripple. The DC link current of each parallel connected module and the total DC link current with and without interleaving at 50kHz switching frequency are shown in Fig. 11. The DC link voltage ripple of each series connected module and the total DC link voltage with and without interleaving are also shown in Fig. 12.

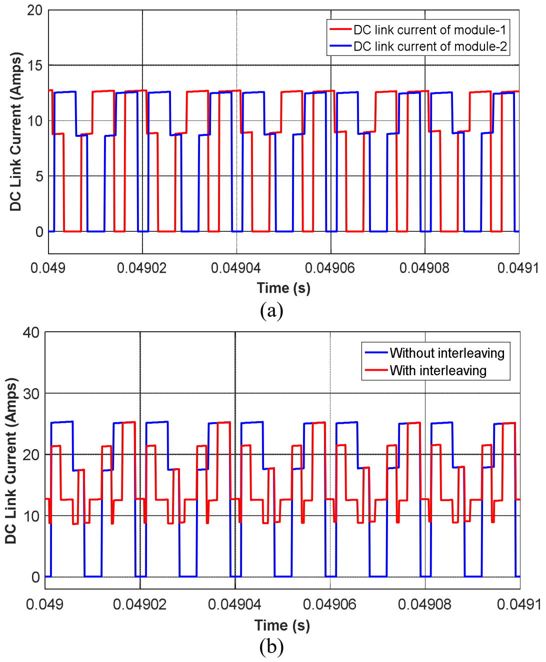

Fig. 11. (a) The DC link current of each module, (b) total DC link current with and without interleaving

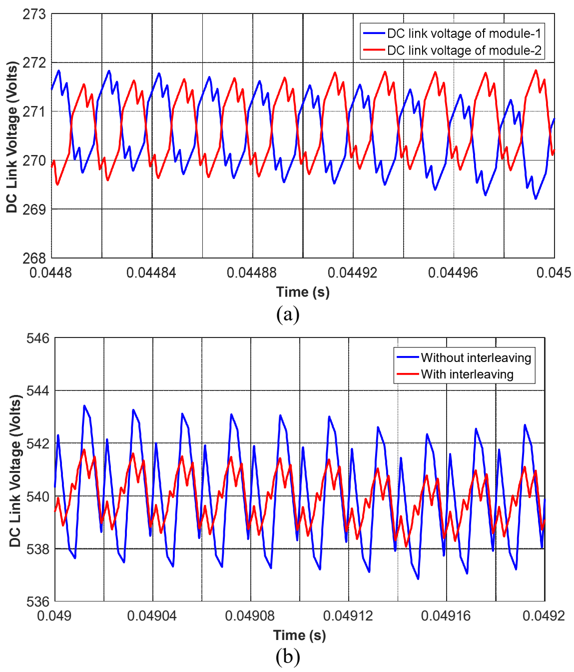

Fig. 12. (a) DC link voltage of each module, (b) Total DC link voltage with and without interleaving

The line-to-line output voltage and line current of one module are shown in Fig. 13. The performance of the proposed IMMD system and its conventional counterpart are listed in Table 5 including the RMS ripple current of each capacitor (I_{crms}), the required capacitance for each capacitor (C_{dc}), required voltage for each capacitor (V_c), number of total capacitors, total harmonic distortion of the line-to-line voltage (*THDv*) and line current (*THDi*). In this analysis, switching frequencies selected for IMMD and conventional motor drive are 50kHz and 20kHz, respectively.

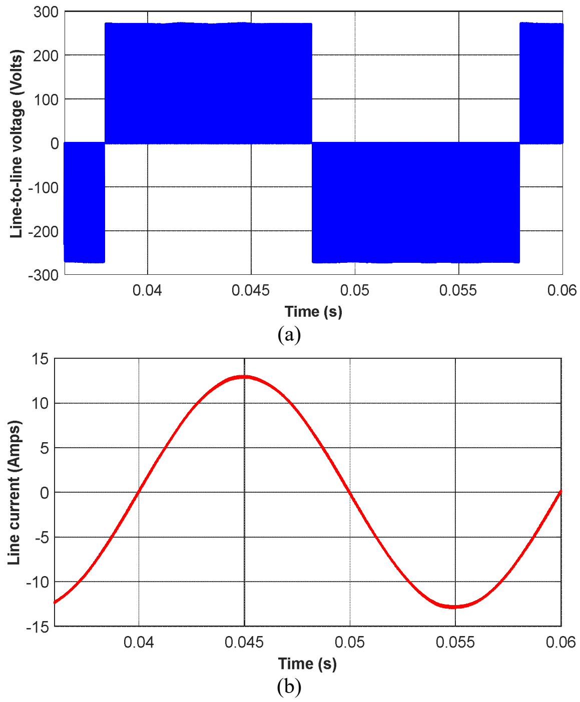

Figure 13. (a) Line-to-line voltage, (b) Line current

The results show that, the required RMS ripple current rating of the capacitors is decreased to almost half with the application of interleaving in the IMMD case. Metallized film capacitors are known to have high current handling capability, therefore decreasing the capacitance requirement is more critical and the most convenient way to achieve this is to increase the switching frequency. However, the current rating does not depend on the switching frequency. The capacitance requirement also decreases almost half of its value with interleaving. It can be further reduced by increasing the switching frequency using GaN devices when IMMD configuration is used. One drawback of using the modular configuration is the necessity of using two capacitor banks due to the series connection. Interleaving between series connected modules does not contribute to reduction of the DC link voltage ripple.

Capacitors from commercially available products are selected for the conventional and proposed systems, parameters of which are listed in Table 6. Using the thermal model, temperature rise of the capacitors is also analyzed and shown in Table 6. Finally, the resultant power density of both the capacitor bank and overall IMMD is analyzed to verify the performance of the design. Using the motor dimensions, PCB dimensions and capacitor heights, the power density of the capacitor bank and overall system (excluding the heat sink) are calculated as 184 kW/lt and 1.1 kW/lt, respectively. This result shows that, the performance criteria defined for the design process have been achieved in terms of power density, efficiency and fault tolerance. The potential drawbacks of the proposed design are the increased complexity of the motor drive control. Active voltage balancing should be applied to the series connected modules in order to avoid voltage mismatch in the case of unbalanced load. Moreover, potential circulating currents between parallel connected modules should be investigated and measures should be taken.

TABLE V
PERFORMANCE OF THE PROPOSED IMMD AND COMPARISON WITH THE CONVENTIONAL SYSTEM

Parameter	Conventional System	Proposed System
$I_{c,rms}$	10.13 A	5.76 A
C_{dc}	97 µF	18 µF
V_c	630 V	300 V
Total capacitor	1	2
THDv	79.91 %	89.15 %
THDi	0.48 %	0. 47 %

TABLE VI
PARAMETERS OF THE SELECTED CAPACITOR BANKS

Parameter	Conventional	Proposed
Voltage	600 V	300 V
Capacitance	100 µF	20 µF
Current	100 A	20 A
ESR	0.9 mΩ	4 mΩ
ESL	25 nH	11 nH
Width/Length	101mm x 101mm	28mm x 42mm
Height	40 mm	37 mm
Total volume	408 cm^3	43.5 cm^3
Thermal resistance	6.9 ^{0}C/W	12 ^{0}C/W
Power loss	92 mW	132 mW
Temperature rise	0.6 ^{0}C	1.6 ^{0}C

V. CONCLUSIONS

In this study, an integrated modular motor drive system is proposed which can replace conventional motor drive systems, and its design process is presented. The proposed system brings several advantages such as increased power density, enhanced fault tolerance and reliability, reduction in EMI problems and voltage stress across devices, and increased surface area for better cooling.

The design is based on 2-level inverter modules which can be connected in series and/or parallel on the DC link thanks to the modular structure. The number of series/parallel modules are determined based on the size reduction of the DC link capacitor with proper interleaving angle, and the available device voltage and current ratings. A PMSM having FSCW stator is designed and a suitable modular winding configuration is proposed. The design of the modular motor drive is based on GaN power FETs selected from two different manufacturers. Loss characterization and analysis is performed using these devices along with a conventional converter in which IGBT is utilized for comparison.

It has been shown that both GaN devices have higher efficiencies even with a switching frequency five times higher than the conventional one. Moreover, DC bus capacitor banks are selected for these systems and the effects of interleaving, which is only applicable for modular structure, to the size of capacitors are presented. It is shown that, an overall system power density higher than 1 kW/lt can be achieved with 98% motor drive efficiency and 96% motor efficiency for an IMMD having 8 kW output power. Considering also the improvements on the system fault tolerance, the performance of the IMMD system has been proven to be successful to replace the conventional motor drive systems using the design process presented here.

VI. ACKNOWLEDGMENT

This work is supported by Scientific and Technological Research Council of Turkey (TUBITAK) under the TUBITAK project number 117E252.

VII. REFERENCES

[1] R. Abebe et al., "Integrated motor drives: state of the art and future trends," *IET Electr. Power Appl.*, vol. 10, no. 8, pp. 757–771, Sep. 2016.

[2] J. J. Wolmarans, M. B. Gerber, H. Polinder, S. W. H. De Haan, J. A. Ferreira, and D. Clarenbach, "A 50kW integrated fault tolerant permanent magnet machine and motor drive," *PESC Rec. - IEEE Annu. Power Electron. Spec. Conf.*, pp. 345–351, 2008.

[3] M. D. Hennen, M. Niessen, C. Heyers, H. J. Brauer, and R. W. De Doncker, "Development and control of an integrated and distributed inverter for a fault tolerant five-phase switched reluctance traction drive," *IEEE Trans. Power Electron.*, vol. 27, no. 2, pp. 547–554, 2012.

[4] J. Wang, Y. Li, and Y. Han, "Integrated Modular Motor Drive Design With GaN Power FETs," *IEEE Trans. Ind. Appl.*, vol. 51, no. c, pp. 3198–3207, 2015.

[5] A. Shea and T. M. Jahns, "Hardware integration for an integrated modular motor drive including distributed control," in *2014 IEEE Energy Conversion Congress and Exposition (ECCE)*, 2014, pp. 4881–4887.

[6] M. Ugur and O. Keysan, "DC link capacitor optimization for integrated modular motor drives," *2017 IEEE 26th Int. Symp. Ind. Electron.*, vol. i, pp. 263–270, 2017.

[7] N. R. Brown, T. M. Jahns, and R. D. Lorenz, "Power Converter Design for an Integrated Modular Motor Drive," *Ind. Appl. Conf. 2007. 42nd IAS Annu. Meet. Conf. Rec. 2007 IEEE*, pp. 1322–1328, 2007.

[8] J. Wang and Y. Han, "A new concept of multilevel converter motor drive with modular design and split winding machine," in *2014 Power and Energy Conference at Illinois (PECI)*, 2014, pp. 1–6.

[9] S. U. Chung, J. M. Kim, D. H. Koo, B. C. Woo, D. K. Hong, and J. Y. Lee, "Fractional slot concentrated winding permanent magnet synchronous machine with consequent pole rotor for low speed direct drive," *IEEE Trans. Magn.*, vol. 48, no. 11, pp. 2965–2968, 2012.

[10] J. Wang, Y. Li, and Y. Han, "Evaluation and design for an integrated modular motor drive (IMMD) with GaN devices," *2013 IEEE Energy Convers. Congr. Expo. ECCE 2013*, no. Immd, pp. 4318–4325, 2013.

[11] E. A. Jones, F. F. Wang, and D. Costinett, "Review of Commercial GaN Power Devices and GaN-Based Converter Design Challenges," *IEEE J. Emerg. Sel. Top. Power Electron.*, vol. 4, no. 3, pp. 707–719, 2016.

[12] J. W. Kolar and S. D. Round, "Analytical calculation of the RMS current stress on the DC-link capacitor of voltage-PWM converter systems," *IEE Proc. - Electr. Power Appl.*, vol. 153, no. 4, p. 535, 2006.

VIII. BIOGRAPHIES

Mesut Uğur received his BSc and MSc degrees from the Department of Electrical and Electronics Engineering, Middle East Technical University, Ankara, Turkey in 2012 and 2015, respectively. He is currently working towards the PhD degree at Middle East Technical University.

He is currently a Research Associate in Middle East Technical University. His main research interest are electric motor drives and renewable energy.

Ozan Keysan received the M.S. degree from the Middle East Technical University, Ankara, Turkey, in 2008, and the Ph.D. degree investigating high-temperature superconducting direct-drive generators for offshore wind turbines at the Institute for Energy Systems at Edinburgh University, Edinburgh, U.K. in 2013.

He is currently an Assistant Professor in Middle East Technical University. His research interests include renewable energy, design and optimization of electrical machines and smart grids.